SECURITY CLASSIFICATION OF THIS PAGE *(When Data Entered)*

REPORT DOCUMENTATION PAGE		READ INSTRUCTIONS BEFORE COMPLETING FORM
1. REPORT NUMBER NRL Report 7662	2. GOVT ACCESSION NO.	3. RECIPIENT'S CATALOG NUMBER
4. TITLE *(and Subtitle)* J INTEGRAL AND THE INITIATION OF CRACK EXTENSION IN A TITANIUM ALLOY		5. TYPE OF REPORT & PERIOD COVERED completes one phase 6. PERFORMING ORG. REPORT NUMBER
7. AUTHOR(s) G. R. Yoder and C. A. Griffis		8. CONTRACT OR GRANT NUMBER(s)
9. PERFORMING ORGANIZATION NAME AND ADDRESS Naval Research Laboratory Washington, D. C. 20375		10. PROGRAM ELEMENT, PROJECT, TASK AREA & WORK UNIT NUMBERS NRL Problem 63M01-24 RR 022-01-46-5431
11. CONTROLLING OFFICE NAME AND ADDRESS Department of the Navy Office of Naval Research Arlington, Va. 22217		12. REPORT DATE February 26, 1974 13. NUMBER OF PAGES 36
14. MONITORING AGENCY NAME & ADDRESS*(if different from Controlling Office)*		15. SECURITY CLASS. *(of this report)* Unclassified 15a. DECLASSIFICATION/DOWNGRADING SCHEDULE

16. DISTRIBUTION STATEMENT *(of this Report)*

Approved for public release; distribution unlimited.

17. DISTRIBUTION STATEMENT *(of the abstract entered in Block 20, if different from Report)*

18. SUPPLEMENTARY NOTES

19. KEY WORDS *(Continue on reverse side if necessary and identify by block number)*

J integral
Elastic-plastic fracture
Crack extension
Fracture
Fracture mechanics
Titanium 6Al-4V alloy

20. ABSTRACT *(Continue on reverse side if necessary and identify by block number)*

Interest in the J integral proposed by Rice stems from its potential to determine the plane strain fracture toughness (K_{Ic}), a material constant, from elastic-plastic laboratory specimens too small to meet the full constraint criteria defined in ASTM-E399-72. J represents an extension of G, the linear elastic fracture mechanics parameter owing to Irwin, to include nonlinear load-displacement response, and as such the critical value J_{Ic} is a criterion proposed for the initiation of crack extension. For J, or J_{Ic}, to be a viable parameter, it is necessary to demonstrate by experiment its independence of specimen geometry, including thickness and initial crack length.

(Continued)

20.

Though previous work of others has shown this to be true for the special case of fully plastic fracture where initiation of crack extension coincided with limit load, the present work is focused on the case where crack extension initiates long before maximum load. This more general case was examined by selecting a Ti-6Al-4V alloy known to be susceptible to sustained-load cracking. Four types of three-point bend specimens (two thicknesses and two crack lengths) were employed. These fatigue-precracked specimens exhibited, to varying degrees, loading behavior characteristic of the lower end of the elastic-plastic regime. For each specimen type, values of the J integral were obtained as a function of crack extension. Values of the J integral were determined on the basis of a compliance-type calibration which used the plane stress solutions of Bucci et al.; these simulated well the loading curves of the fatigue-precracked specimens. For each specimen type, crack extensions were defined by unloading duplicate specimens from various points on the load-displacement diagram, followed by heat-tinting.

The results from all four specimen types suggest that the J-integral value associated with a given amount of crack extension is independent of specimen thickness and crack length. For various criteria examined for the initiation of crack extension, the resultant J_{Ic} numbers were in good agreement with an ASTM-valid K_{Ic} number obtained for this material.

CONTENTS

J INTEGRAL AND THE INITIATION OF CRACK EXTENSION IN A TITANIUM ALLOY

INTRODUCTION

Significance of the J Integral

Interest in the J integral recently proposed by Rice [1] stems from its potential to determine the plane-strain fracture toughness (K_{Ic}), a material constant, from elastic-plastic or fully plastic laboratory specimens which are too small to meet the full constraint criteria defined in ASTM-E399-72 [2]. The parameter J represents an extension of G, the linear elastic fracture mechanics parameter owing to Irwin [3], to include nonlinear load-displacement response, and, as such, J is a criterion for the initiation of crack extension.

State of the Art in Experimentally Validating J

Little has been reported thus far concerning experimental validation of the J integral as a criterion for initiation of crack extension. Although Srawley [4], Kobayashi et al. [5], Ke and Liu [6], McCabe [7], and others have examined various aspects of the J integral experimentally, the work by Begley and Landes [8,9] with rotor and pressure vessel steels represents the primary experimental validation of the J integral. They reported J independence of specimen geometry and agreement between the critical value of the J integral for crack extension (J_{Ic}), as measured from small fully plastic specimens 1/2 in. (1.27 cm) to 2 in. (5.08 cm) thick and the value of G_{Ic} as determined from K_{Ic} testing of plates 8 in. (20.32 cm) and 12 in. (30.48 cm) thick. In these fully plastic specimens, crack extension was reported to initiate at maximum load, thus greatly facilitating the determination of J_{Ic}. However, for many materials, crack extension in the elastic-plastic state initiates prior to the attainment of maximum load, and it is the determination of this initiation point which poses perhaps the major obstacle to measuring J_{Ic} values.

Statement of Approach

It is to this more general case that the present investigation is addressed. The small elastic-plastic specimens examined are from an alloy of the Ti-6Al-4V system, known to be susceptible to subcritical crack growth under sustained load conditions in ambient air [10]. To gain a preliminary assessment as to the relevance of the J integral (and thus J_{Ic}) to the initiation of crack extension, the value of the J integral is determined as a function of crack extension, for three-point bend specimens of different thicknesses and crack lengths.

Manuscript submitted September 24, 1973.

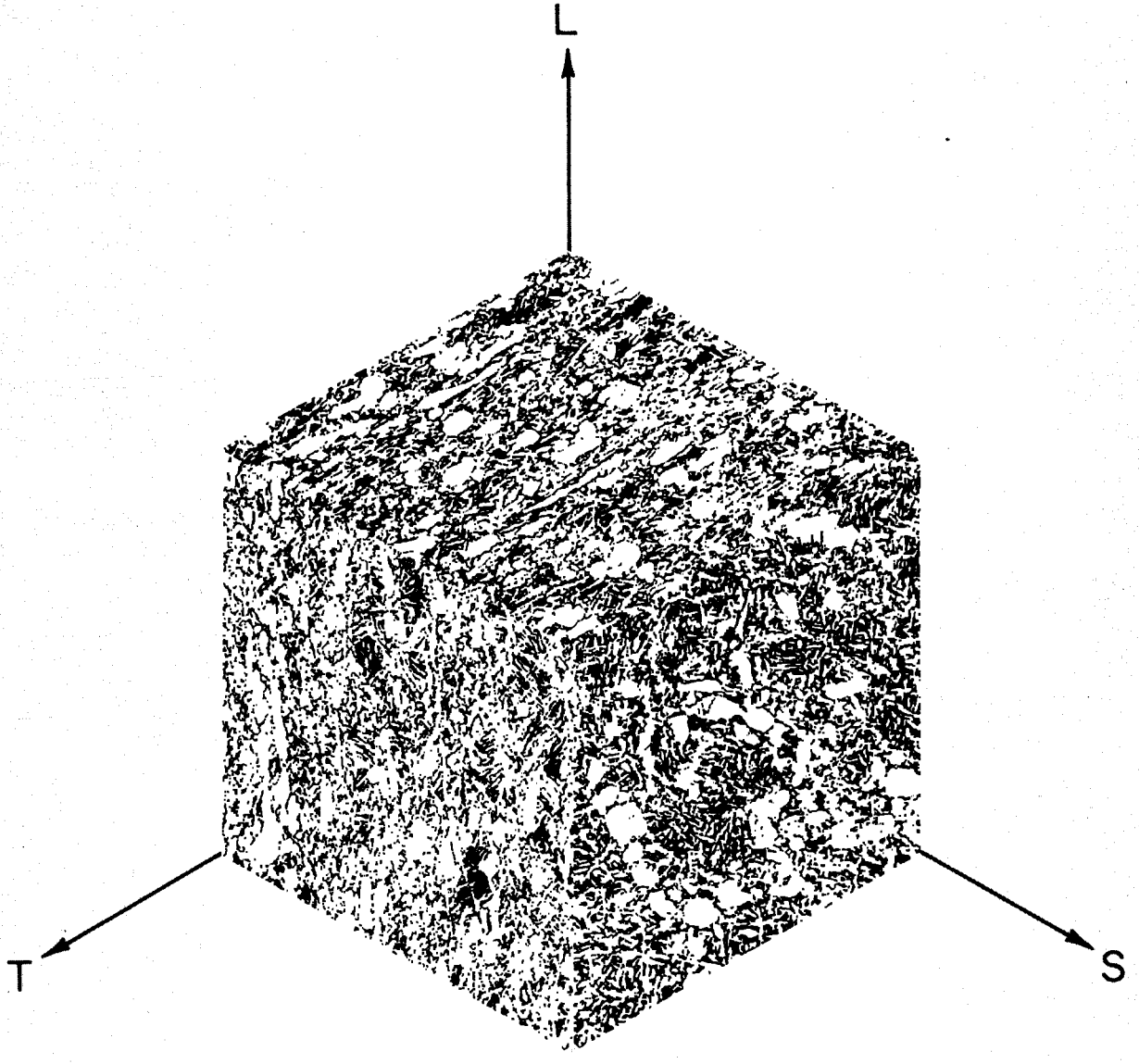

Fig. 1 — Light micrographs of the alloy microstructure (X200)

MATERIAL CHARACTERIZATION

Material used in this investigation was taken from a 1-in.-thick (2.54-cm-thick) plate of mill-annealed Ti-6Al-4V alloy, with the chemical composition given in Table 1. Light photomicrographs (Fig. 1) reveal a microstructure consisting of elongated primary α grains dispersed in an α-β Widmanstatten (basketweave) matrix. Extensive crossrolling is evident from these micrographs and seems to be reflected in the tensile properties shown in Table 2, determined with standard 0.505-in.-diameter (1.28-cm-diameter) tension specimens. The yield strength in both the longitudinal (L) and transverse (T) directions is 124 ksi (866 MPa); Young's modulus is 18.55 X 10^3 ksi (129 GPa) in the T direction.

Table 1
Chemical Composition of the Material Used (NRL Alloy R-14A)

Element	Content (wt-%)
Al	6.0
V	4.1
Fe	0.05
C	0.023
N	0.008
H	0.005
O	0.06

Table 2
Tensile Properties of the Material Used (Table 1)

0.2% Yield Strength		Tensile Strength		Reduction in Area (%)	Elongation (%)	Young's Modulus	
ksi	MPa	ksi	MPa			10^3 ksi	GPa
Transverse Direction (T)							
124.4	868.3	133.8	933.9	39.5	13.5 (in 2 in.)	18.55	129.5
Longitudinal Direction (L)							
124.1	866.2	130.5	910.9	39.5	16.5 (in 1.4 in.)	18.56	129.5

DEFINITION OF THE J INTEGRAL

Path-Independent Contour Integral

The J integral has been proposed to characterize a load-versus-displacement response which is linear for stress states inside a yield surface and nonlinear for those outside. It is defined as an energy line integral for a two-dimensional deformation field by [1]

$$J = \int_{\Gamma} \left(W\, dy - \mathbf{T} \cdot \frac{\partial \mathbf{u}}{\partial x}\, ds \right), \tag{1}$$

where Γ is any contour surrounding the notch or crack tip (Fig. 2); W is the strain energy density,

$$W = W(\epsilon_{mn}) = \int_0^{\epsilon_{mn}} \sigma_{ij}\, d\epsilon_{ij}; \tag{2}$$

$\mathbf{T}$ is the traction vector defined with respect to the outward normal $\mathbf{n} = (dy/ds)\,\hat{i} - (dx/ds)\,\hat{j}$ along Γ, $\mathbf{T} \equiv \boldsymbol{\sigma} \cdot \mathbf{n}$, where $\boldsymbol{\sigma}$ is the stress tensor; $\mathbf{u} = u\hat{i} + v\hat{j}$ is the displacement vector; and ds is an increment of arc length along Γ. To demonstrate path independence of the J integral, Rice considers a closed loop Γ^* which encloses an area A^*. With the application of Green's theorem, Eq. (1) is transformed to an area integral; thus, in Cartesian coordinates,

$$\oint_{\Gamma^*} \left[\left(W - \sigma_{xx} \frac{\partial u}{\partial x} - \sigma_{xy} \frac{\partial v}{\partial x} \right) dy + \left(\sigma_{xy} \frac{\partial u}{\partial x} + \sigma_{yy} \frac{\partial v}{\partial x} \right) dx \right]$$

$$= \iint_{A^*} \left[-\frac{\partial}{\partial y} \left(\sigma_{xy} \frac{\partial u}{\partial x} + \sigma_{yy} \frac{\partial v}{\partial x} \right) + \frac{\partial}{\partial x} \left(W - \sigma_{xx} \frac{\partial u}{\partial x} - \sigma_{xy} \frac{\partial v}{\partial x} \right) \right] dx\,dy. \tag{3}$$

With use of Eq. (2), $\partial W/\partial x$ can be expressed as

$$\frac{\partial W}{\partial x} = \sum_{i,j=1}^{2} \frac{\partial W}{\partial \epsilon_{ij}} \frac{\partial \epsilon_{ij}}{\partial x} = \sum_{i,j=1}^{2} \sigma_{ij} \frac{\partial \epsilon_{ij}}{\partial x}. \tag{4}$$

Using the definition of ϵ_{ij}, the equilibrium equations, and that $\sigma_{ij} = \sigma_{ji}$, Eq. (4) reduces to

$$\frac{\partial W}{\partial x} = \frac{\partial}{\partial x} \left(\sigma_{xx} \frac{\partial u}{\partial x} + \sigma_{xy} \frac{\partial v}{\partial x} \right) + \frac{\partial}{\partial y} \left(\sigma_{xy} \frac{\partial u}{\partial x} + \sigma_{yy} \frac{\partial v}{\partial x} \right). \tag{5}$$

Thus the integrand in Eq. (3) vanishes, proving path independence. Hence the contour Γ can be chosen remote from the crack tip.

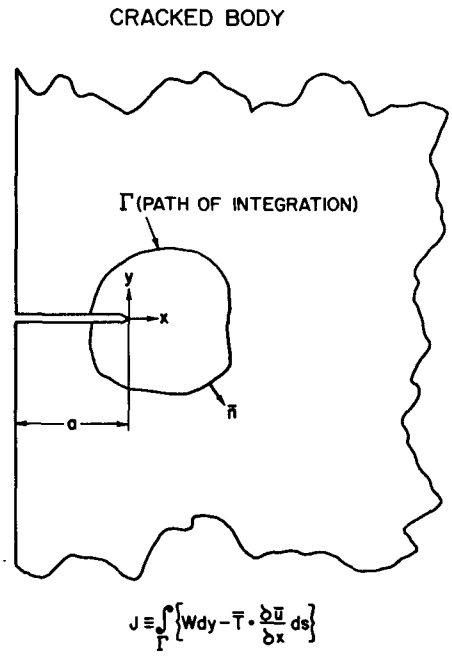

Fig. 2 — Arbitrary line-integral contour Γ surrounding a crack tip, with designated coordinates

Energy-Rate Interpretation

It has been shown by Rice [11] and Irwin [12] that the J integral is equivalent to

$$J = \frac{-dU}{da}, \tag{6}$$

where a is the crack length and U is given by

$$U = \iint_A W \, dxdy - \int_\Gamma \mathbf{T} \cdot \mathbf{u} \, ds, \tag{7a}$$

or

$$dU = da \iint_A \frac{\partial W}{\partial a} \, dxdy - \int_\Gamma \mathbf{T} \cdot \mathbf{du} \, ds. \tag{7b}$$

Rice designates dU as the difference in potential energy per unit thickness between two identically loaded bodies (specimens) which are similar in every respect except for an incremental difference in crack length (da). Since

$$\mathbf{du} = \frac{\partial u}{\partial a} da \hat{i} + \frac{\partial v}{\partial a} da \hat{j} \tag{8}$$

and da = −dx, then

$$dU = -da \iint_A \frac{\partial W}{\partial x}\, dx dy$$

$$-\int_\Gamma \left[\left(\sigma_{xx}\frac{dy}{ds} - \sigma_{xy}\frac{dx}{ds}\right)\hat{i} + \left(\sigma_{xy}\frac{dy}{ds} - \sigma_{yy}\frac{dx}{ds}\right)\hat{j}\right] \cdot \left(\frac{\partial u}{\partial a}da\hat{i} + \frac{\partial v}{\partial a}da\hat{j}\right) ds$$

$$= -da \int_\Gamma \left[\left(W - \sigma_{xx}\frac{\partial u}{\partial x} - \sigma_{xy}\frac{\partial v}{\partial x}\right) dy + \left(\sigma_{xy}\frac{\partial u}{\partial x} + \sigma_{yy}\frac{\partial v}{\partial x}\right) dx\right]. \quad (9)$$

The integrand in Eq. (9) is thus the same as in Eq. (1). Hence J is simply an extension of G to include nonlinear behavior. (The formulation of G as a path-independent integral, equivalent to J, was first proposed by Sanders [13].) In the linear case, J is the crack extension force, da is interpreted as an increment of crack extension, and dU is interpreted as the potential energy of the cracked specimen. For the nonlinear case, these interpretations no longer hold, since one of the limitations of nonlinear elasticity theory is that unloading be prohibited.

It is hypothesized that J_{Ic} will be a material constant for the initiation of crack extension, whether the specimen used for its determination is linear elastic (fully constrained crack) or is nonlinear (such as a smaller specimen, with the constraint relaxed) at the point of initiation. Therefore J_{Ic} should be related to parameters of linear elastic fracture mechanics by

$$J_{Ic} = G_{Ic} = K_{Ic}^2\left(\frac{1-\nu^2}{E}\right), \quad (10)$$

where material constants G_{Ic} and K_{Ic} are the critical crack-extension force and the critical stress-intensity factor respectively, ν is Poisson's ratio, and E is Young's modulus. It is debatable however as to whether the term $1 - \nu^2$ might better be omitted from this equation [14-16].

THE MEASUREMENT OF J

Rice [1] suggested that the compliance testing technique of linear elastic fracture mechanics is directly extensible through Eq. (6) to elastic-plastic materials; also, he suggested that highly approximate analyses can be used, since the determination of J requires only overall changes in compliance. Begley and Landes [8,9], following the suggestion of Rice [11], developed the experimental technique illustrated in Fig. 3 to measure J in nonlinear materials. This method makes use of the fact that for specimens (of differing crack lengths a) loaded to a constant displacement δ, that is, $J = -(dU/da)_{\delta=const}$, the potential energy U is simply the area under the load-versus-displacement diagram. They were able to obtain their J(a)-versus-δ calibrations using fatigue-precracked specimens, inasmuch as the initiation of crack extension could not be detected prior to the onset of plastic instability (the attainment of maximum load). On the other hand a J(a)-versus-δ calibration can be formed from load-versus-displacement records generated analytically from the plane-stress solutions of Bucci et al. [17]. Using this procedure, Bucci et al.

estimated values of J_{Ic} which agreed quite well with the Begley-Landes results. Before the calibration procedure used in the present work is described, the specimens and test methods will be described.

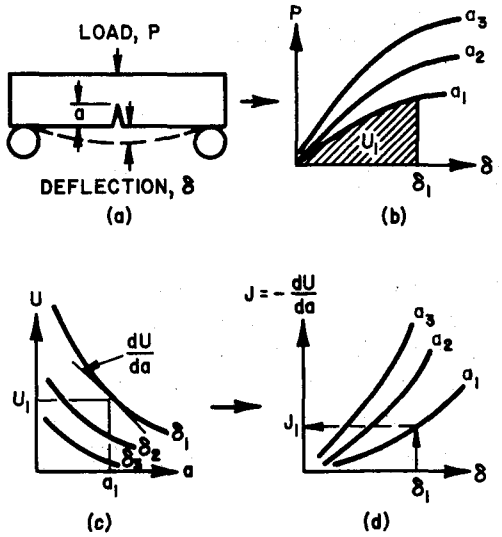

Fig. 3 — Graphical method for determining J(a) vs δ. The load-displacement response of three-point bend bars, as measured in (a), is recorded in (b) for specimens of various crack lengths a. Graphical integration of the areas under the curves in (b) gives the potential energy U as plotted in (c) versus crack length a for various deflections δ. Graphical differentiation of constant-displacement curves in (c) gives $J = -(dU/da)_{\delta=const}$, thus yielding the compliance calibration curves J(a) vs δ shown in (d).

Specimens and Test Methods

Studies were made with the three-point bend bar sketched in Fig. 4. Thicknesses B were either 0.500 in. (1.27 cm) or 1.000 in. (2.54 cm), both cut from nominally 1-in.-thick plate. Fatigue precracks were nominally either a = 0.685 in. (1.74 cm), so that a/W = 0.685/1.500 = 0.45, or a = 0.885 in. (2.25 cm), so that a/W = 0.59. All testing was at room temperature in the fixture shown in Fig. 5. The displacement δ was measured between the knife blades shown in Fig. 5a, a measurement similar in nature to the "ram travel" employed by Begley and Landes. The machine contribution to this displacement was approximately linear with load and with magnitude of ≈0.0041 in./10 kips (0.104 mm/44.45 kN). In this fixture the span between rollers was S = 5.975 in. (15.18 cm), or S/W = 3.98. The loading rate employed for the specimens with B = 1.000 in. (2.54 cm) was 1.5 kips/min (6.67 kN/min), with proportionate reduction for the lesser thickness. Supplementary clip-gage measurements of the crack mouth opening deflection (CMOD) were made, as described in ASTM-E399-72 [2] and shown in Fig. 5b.

Calibration Procedure

In the present work it was deemed undesirable to use fatigue-precracked specimens to determine a calibration of J(a) versus δ, since the initiation of crack extension might well be expected long before the attainment of maximum load, owing to alloy susceptibility to sustained load cracking [10]. Instead the elastic-plastic plane stress solution of Bucci et al. was employed to generate a J-versus-δ calibration. The loading curves generated by this method simulate reasonably well the experimental load-displacement behavior using fatigue-precracked specimens; that is, they simulate the experimental loading curves up to the initiation of crack extension, at approximately which point they depart to simulate

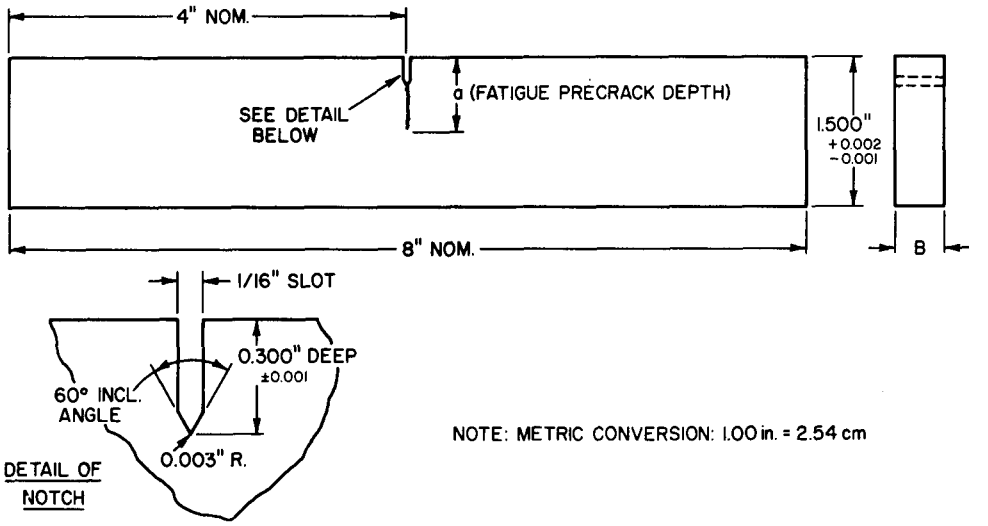

Fig. 4 — Geometry of the three-point bend bars

the behavior had initiation not occurred in the precracked specimen. This can be seen from examination of Fig. 6, which presents data for specimens of thicknesses B = 0.500 and 1.000 in. (1.27 and 2.54 cm) and crack lengths a = 0.685 and 0.885 in. (1.74 and 2.25 cm). In general, however, precise simulation of the experimental loading curves is not mandatory, as it is the change in load-displacement behavior with crack length that would be expected to be of prime importance [16,17]. In the present case the apparent precision in simulating the loading curves with the plane-stress solution is somewhat fortuitous, since the experimental curves include a small (but not negligible) machine contribution to the measured δ.

The J-versus-δ calibration used for analysis of precracked specimens was obtained by applying the procedure outlined in Fig. 3 to the load-versus-displacement curves calculated for a/W ratios of 0.260, 0.343, 0.433, 0.522, 0.613, and 0.702. These load-versus-displacement traces were integrated graphically with use of the trapezoidal rule, using 0.005-in. (0.127-mm) increments of displacement. Slopes of the curves of potential energy U versus δ were taken using increments of 0.050 in. (1.27 mm) in crack length.

Calculation of Elastic-Plastic Loading Curves

To compute load-versus-displacement traces according to the method of Bucci et al. [17] for three-point bend bars, Castigliano's theorem is employed to obtain displacement of the specimen from

$$\delta_s = \frac{\partial E_{tot}}{\partial P}, \tag{11}$$

where E_{tot} is total strain energy stored in a cracked bend bar at load P. Now

$$E_{tot} = E_{\text{no crack}} + E_{\text{due to crack}} \tag{12}$$

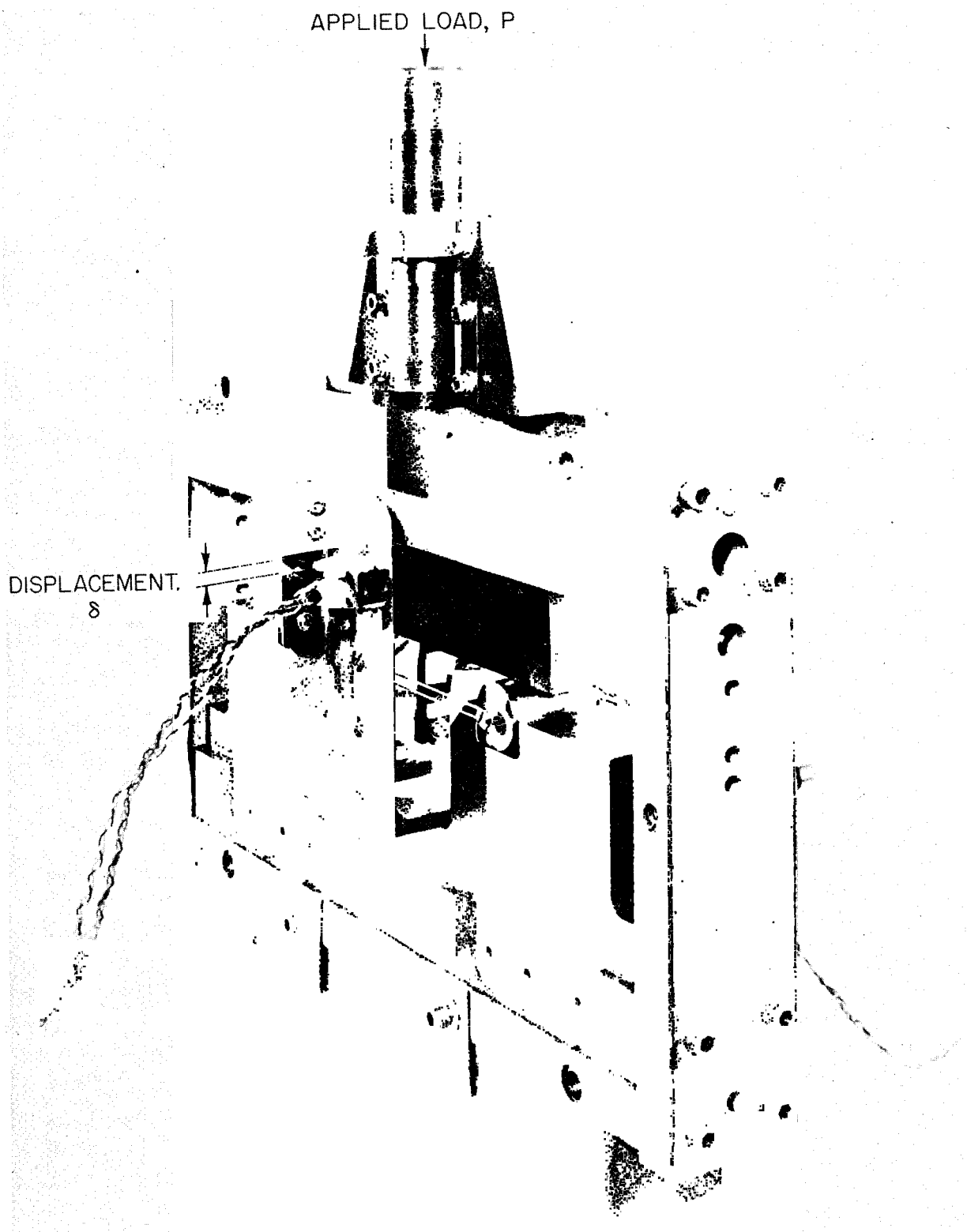

(a) Front view, showing the gage used to measure the displacement δ

Fig. 5 — Specimen mounted in the three-point bend fixture with appended clip gages

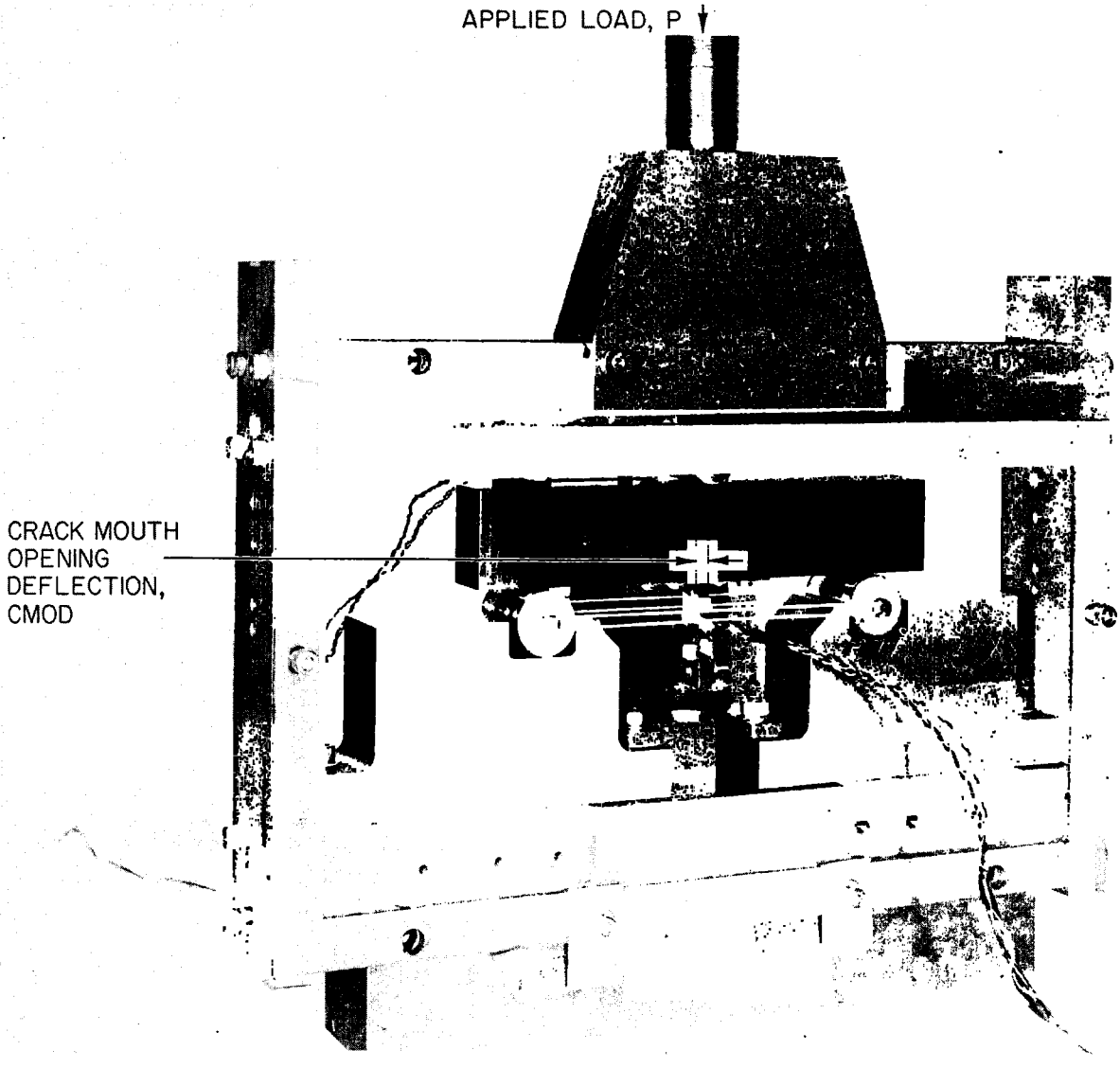

(b) Rear view, showing the gage used to measure the crack mouth opening deflection (CMOD)

Fig. 5 — Specimen mounted in the three-point bend fixture with appended clip gages

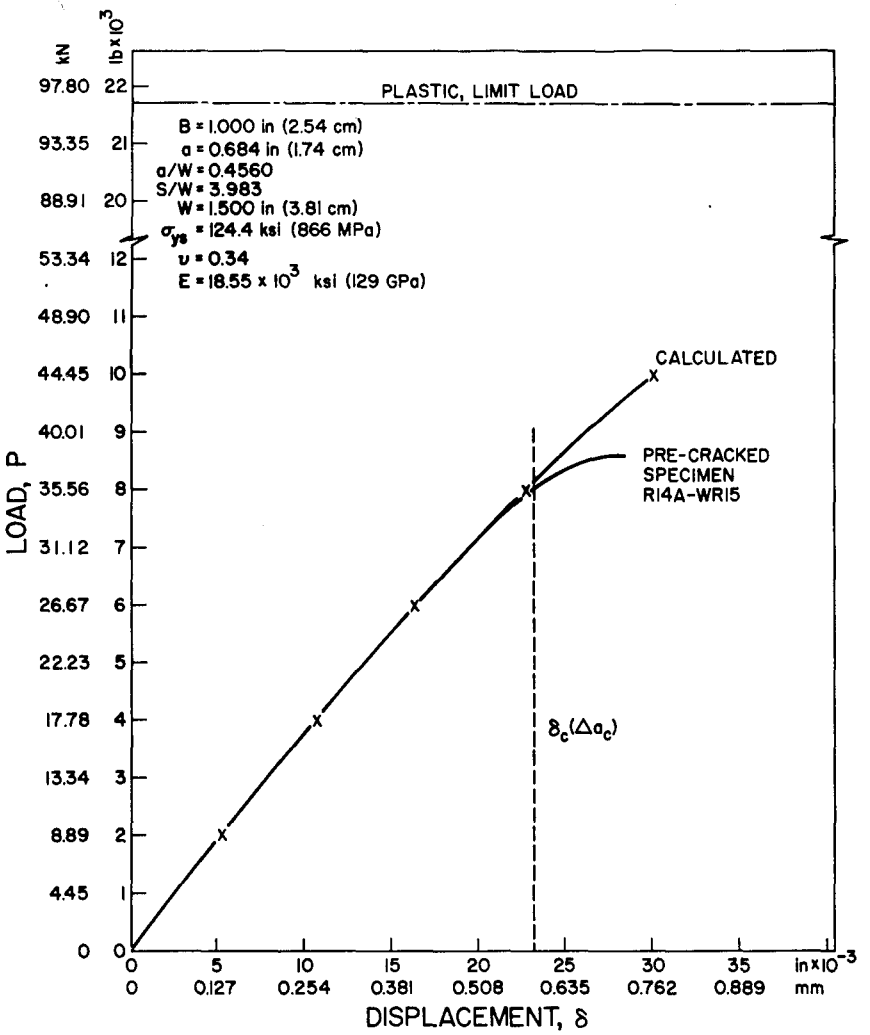

Fig. 6a — Comparison of experimental load-versus-displacement records of precracked specimens with calculated curves for thickness B = 1.000 in. (2.54 cm) and crack length a = 0.684 in. (1.74 cm)

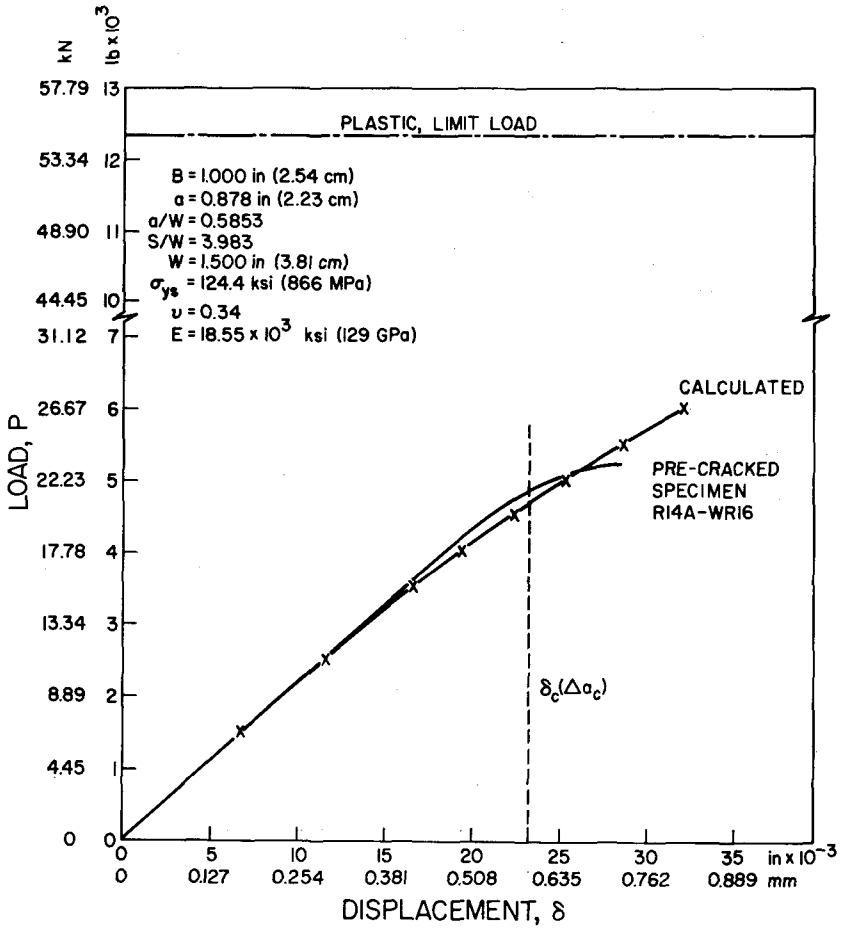

Fig. 6b — Comparison of experimental load-versus-displacement records of precracked specimens with calculated curves for thickness B = 1.000 in. (2.54 cm) and crack length a = 0.878 in. (2.23 cm)

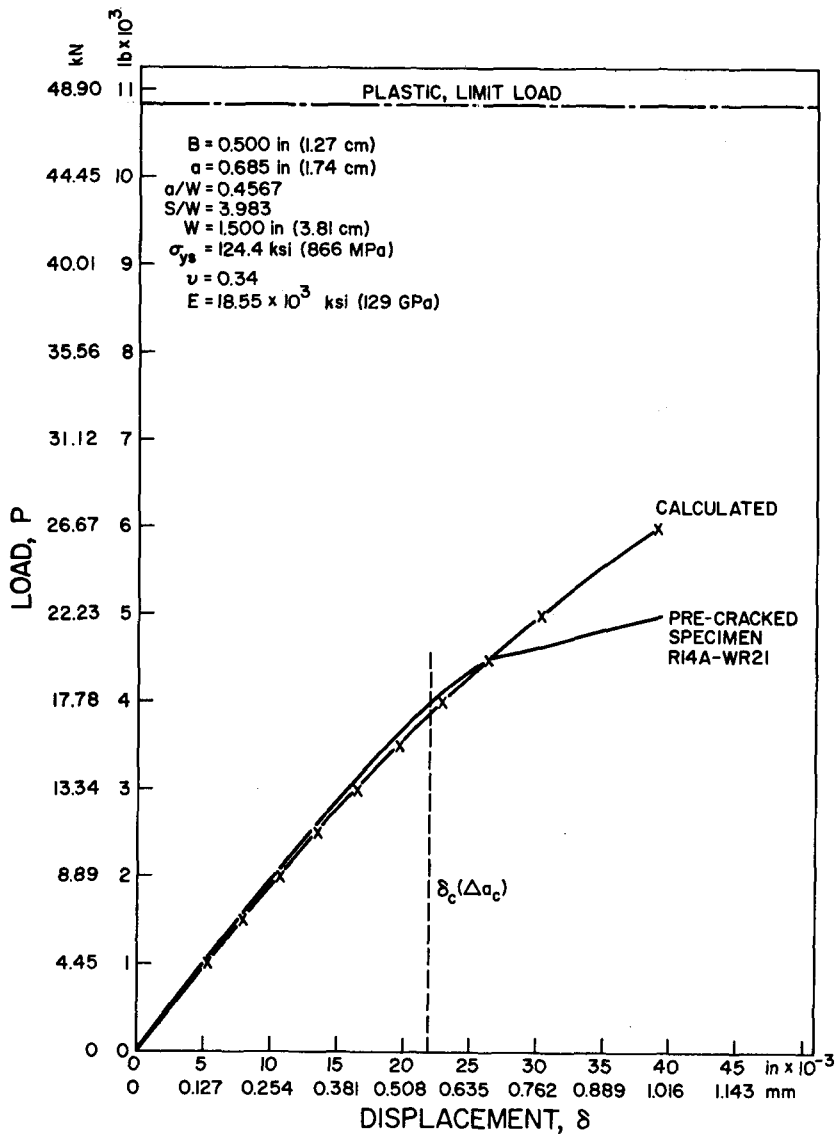

Fig. 6c — Comparison of experimental load-versus-displacement records of precracked specimens with calculated curves for thickness B = 0.500 in. (1.27 cm) and crack length a = 0.685 in. (1.74 cm)

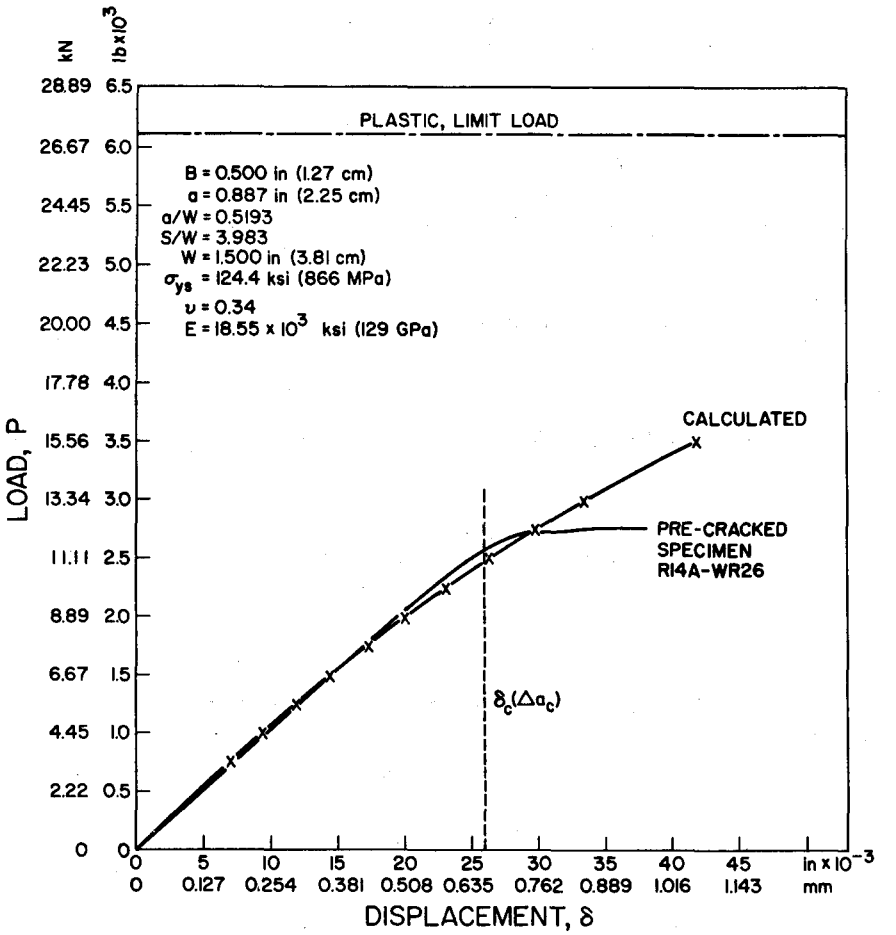

Fig. 6d — Comparison of experimental load-versus-displacement records of precracked specimens with calculated curves for thickness B = 0.500 in. (1.27 cm) and crack length a = 0.887 in. (2.25 cm)

where $E_{no\ crack}$ is computed from strength of materials theory and

$$E_{due\ to\ crack} = B\int_0^a G\ da = \frac{B}{E'}\int_0^a K^2\ da, \tag{13}$$

in which $E' = E$ for plane stress, $E' = E/(1 - \nu^2)$ for plane strain, and K is given by

$$K = \frac{PS}{B(W)^{3/2}}\left[2.9\left(\frac{a}{W}\right)^{1/2} - 4.6\left(\frac{a}{W}\right)^{3/2} + 21.8\left(\frac{a}{W}\right)^{5/2} - 37.6\left(\frac{a}{W}\right)^{7/2} + 38.7\left(\frac{a}{W}\right)^{9/2}\right]. \tag{14}$$

Thus for purely elastic loading the displacement is given by

$$\delta_s = \frac{0.24PS^3}{BEW^3}\ [1.04 + 3.28\ (W/S)^2\ (1 + \nu)] + \frac{2PS^2}{BE'W^2}\left(\frac{a}{W}\right)\left[4.21\left(\frac{a}{W}\right) - 8.89\left(\frac{a}{W}\right)^2 + 36.9\left(\frac{a}{W}\right)^3 - 83.6\left(\frac{a}{W}\right)^4 + 174.3\left(\frac{a}{W}\right)^5 - 284.8\left(\frac{a}{W}\right)^6 + 387.6\left(\frac{a}{W}\right)^7 - 322.8\left(\frac{a}{W}\right)^8 + 149.8\left(\frac{a}{W}\right)^9\right]. \tag{15}$$

To obtain loading curves with a plastic-zone-size (r_y) adjustment, a/W in the above equations is replaced by

$$\left(\frac{a}{W}\right)_{eff} = \frac{1}{W}\ (a + r_y)\ = \frac{1}{W}\left[a + \frac{1}{\alpha\pi}\left(\frac{K}{\sigma_{ys}}\right)^2\right], \tag{16}$$

where $\alpha = 2$ for plane stress and $\alpha = 6$ for plane strain.

THE MEASUREMENT OF CRACK EXTENSION

Heat-Tinting Technique

To determine the point on a load-versus-displacement diagram at which crack extension initiated, several precracked specimens of identical thickness and initial precrack length were loaded to various points on the load-versus-displacement diagram (anywhere from the incidence of nonlinearity to maximum load), followed by complete unloading (Fig. 7). Specimens were then heat tinted in a circulating air furnace at 600°F (589 K) for 2 hours.

Finally specimens were broken open dynamically at low temperature for subsequent examination. Initial fatigue-precrack length was measured as described in ASTM-E399-72, as was the crack extension delineated by heat tinting; that is, the amount of crack extension was taken as an average of that measured at the quarterpoints of specimen thickness. Inasmuch as the initiation of crack extension is a heterogeneous nucleation process, this is admittedly an arbitrary measure of crack extension and therefore should be kept in mind as a potential source of scatter in results to be presented in subsequent sections. Uncertainty in individual measurements is ≈±0.001 in. (0.025 mm).

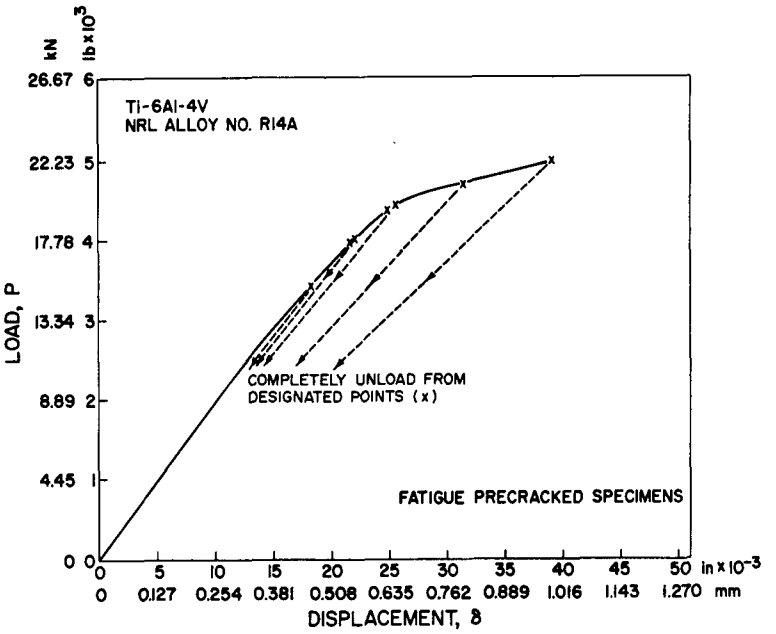

Fig. 7 — Unloading points chosen from the load-versus-displacement diagram to examine for the amount of crack extension; for the case illustrated B = 0.500 in. (1.27 cm) and a = 0.685 in. (1.74 cm)

Photographic Documentation

Since the measure of crack extension is arbitrary, photographic documentation of most of the fracture surfaces is shown in Figs. 8 and 9. It is evident from these figures that, particularly at the greater crack extensions, the crack front at the point of unloading has an undulated shape, symmetric about the midthickness. This shape suggests that resistance to crack extension is less at the 1/4 and 3/4 points through the specimen thickness than at the midpoint.

The mode of crack extension in this alloy is microvoid coalescence, as illustrated by the replica electron micrograph in Fig. 10.

Other Methods

Alternative methods have been suggested by others and considered for determination of the point of initiation of crack extension in the present work:

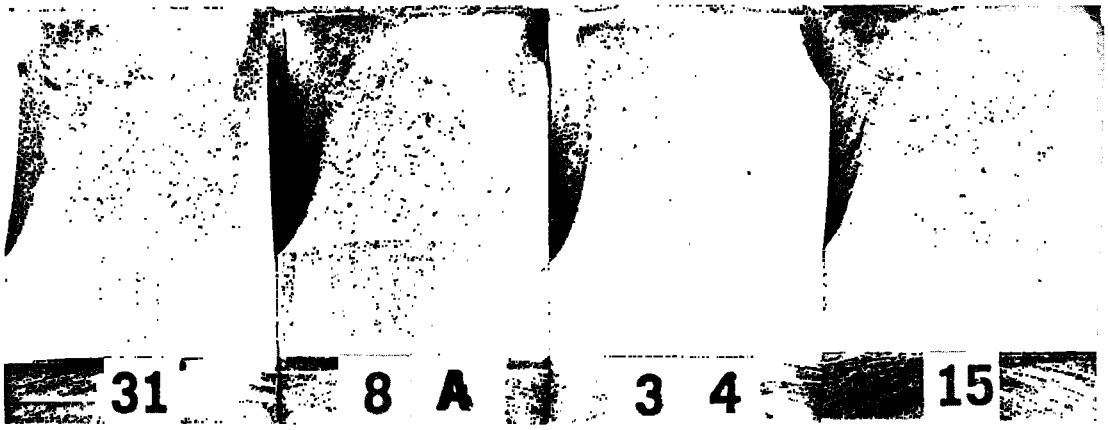

(a) a = 0.685 in. (1.74 cm)

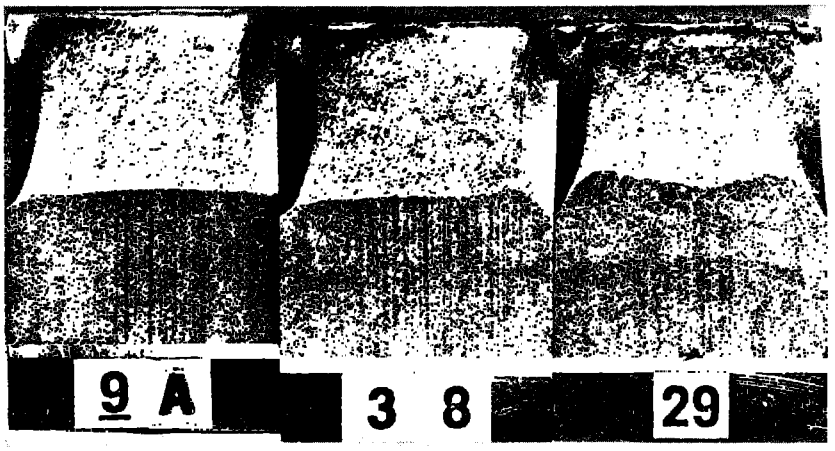

(b) a = 0.885 in. (2.25 cm)

Fig. 8 — Macrofractographic documentation of crack extension, for plate thickness B = 1.000 inch (2.54 cm)

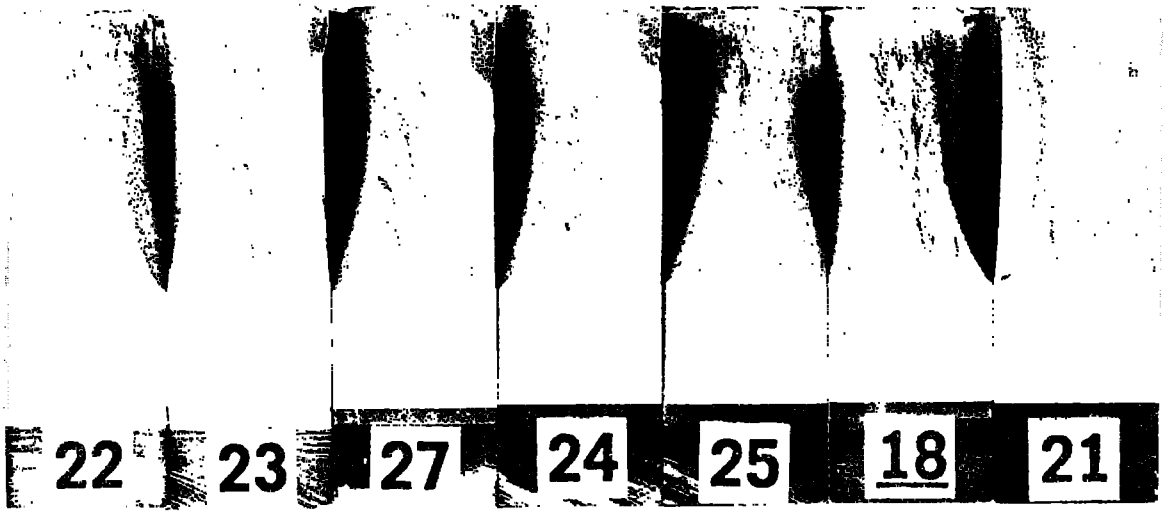

(a) a = 0.685 in. (1.74 cm)

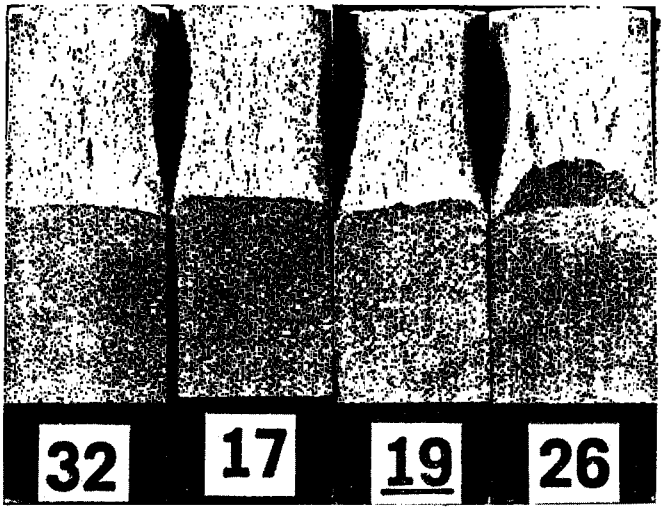

(b) a = 0.885 in. (2.25 cm)

Fig. 9 — Macrofractographic documentation of crack extension, for plate thickness B = 0.500 inch (1.27 cm)

Fig. 10 — Mode of crack extension, as indicated by a replica electron fractograph (X 4240)

- The point at which the loading curve of a fatigue-precracked specimen deviates from a notched curve of equivalent "crack length" would be an attractive criterion for initiation but did not meet with success in the present work.

- If a specimen were unloaded a few percent at successively greater loads, then the unloading slopes may indicate initiation. This approach also failed to succeed.

- Deviation of the precracked curves from those generated by the technique of Bucci et al. might indicate initiation.

J INTEGRAL AND THE INITIATION OF CRACK EXTENSION

The results suggest that the J integral, as a function of crack extension, is independent of specimen thickness and initial crack length. Four criteria for the initiation of crack extension have been used to define the critical value of the J integral $J_{Ic}(\Delta a)$. Three of these are based on a specific percentage of crack extension (0, 1 and 2%); the fourth is based on an apparent correlation between percent secant offset of the crack mouth opening deflection (CMOD), referenced to the point of unloading, and the absolute amount of crack extension. The values of $J_{Ic}(\Delta a)$ so determined from elastic-plastic specimens are in reasonable agreement with an ASTM-valid K_{Ic} number obtained for this material. The value of $J_{Ic}(\Delta a)$ determined at initiation appears to be only about 1/3 of the value implied if the displacement δ at maximum load were used.

Establishment that the J Integral is Independent of B and a, and the Definition of J_{Ic}

Percent CMOD Secant Offset as an Initiation Criterion

Figure 11 shows values of the J integral plotted as a function of crack extension Δa. The data points from the various thicknesses B and crack lengths a examined appear to fall in a band, surprisingly narrow in view of the somewhat arbitrary measure of crack extension Δa employed. These results suggest that the J integral for a given amount of crack extension is independent of thickness and crack length. Of course J may not be a meaningful parameter after the initiation of crack extension.

Scatter in this figure and the next is attributable not only to the measurement of Δa and the graphical integration procedures etc. used to obtain the J-versus-δ calibration but also to inhomogeneity in the plate itself.

Inasmuch as the Begley and Landes work regarding experimental verification of the J integral focused on maximum load as the initiation point, it is worth noting that the values of J at maximum load J_{Pmax} indicated in Fig. 11 are some 2 to 3 times greater than $\lim J(\Delta a)$ as $\Delta a \rightarrow 0$. Furthermore there is a discrepancy in J_{Pmax} implied from various (B, a) combinations; an example is $J_{Pmax} = 0.617$ ksi·in. (109 kPa·m) for B = 0.500 in. (1.27 cm) versus $J_{Pmax} = 0.341$ ksi·in. (60 kPa·m) for B = 1.000 in. (2.54 cm) (both for a = 0.685 in. (1.74 cm)).

In Fig. 12 the percent CMOD secant offset is plotted as a function of Δa. The relationship appears to be approximately linear and independent of thickness and initial crack length. In K_{Ic} testing, the 5% CMOD secant offset is used to define the point of initiation (Δa_c). If in the present case the 5% CMOD secant offset is taken to infer that $\Delta a_c \approx 9.5$ mils (0.24 mm) from Fig. 12, then, by relating this value of Δa_c back to Fig. 11, the value of J_{Ic} so inferred appears to lie between 192 and 250 psi·in. (34.0 and 44.3 kPa·m). When the conversion $J = G = K^2/E$ is employed, this value of J_{Ic} implies that K_{Ic} lies between 59.6 and 68.1 ksi·$\sqrt{\text{in.}}$ (66.3 and 75.8 MPa·$m^{1/2}$ respectively) as indicated in the diagram. Thus the uncertainty in K_{Ic} and J_{Ic}, as determined by this method, is of similar order as the toughness variation which would be expected in the plate itself [18].

As an alternative to the percent secant offset of the CMOD, the percent secant offset in δ at the point of unloading was examined as a measure of crack extension. The results (Fig. 13) when compared to those in Fig. 12, suggest that percent secant offset in δ is not as precise a measure of crack extension as the percent secant offset of the CMOD, especially in the region of initiation.

It is not meant to be inferred from the data in Fig. 12 that for every alloy, regardless of fracture state, the 5% CMOD secant offset can usefully define initiation. For the fully plastic state this would not be expected. However these data do suggest that this criterion is extensible beyond the bounds of elastic, plane-strain fracture, well into the nonlinear elastic-plastic range.

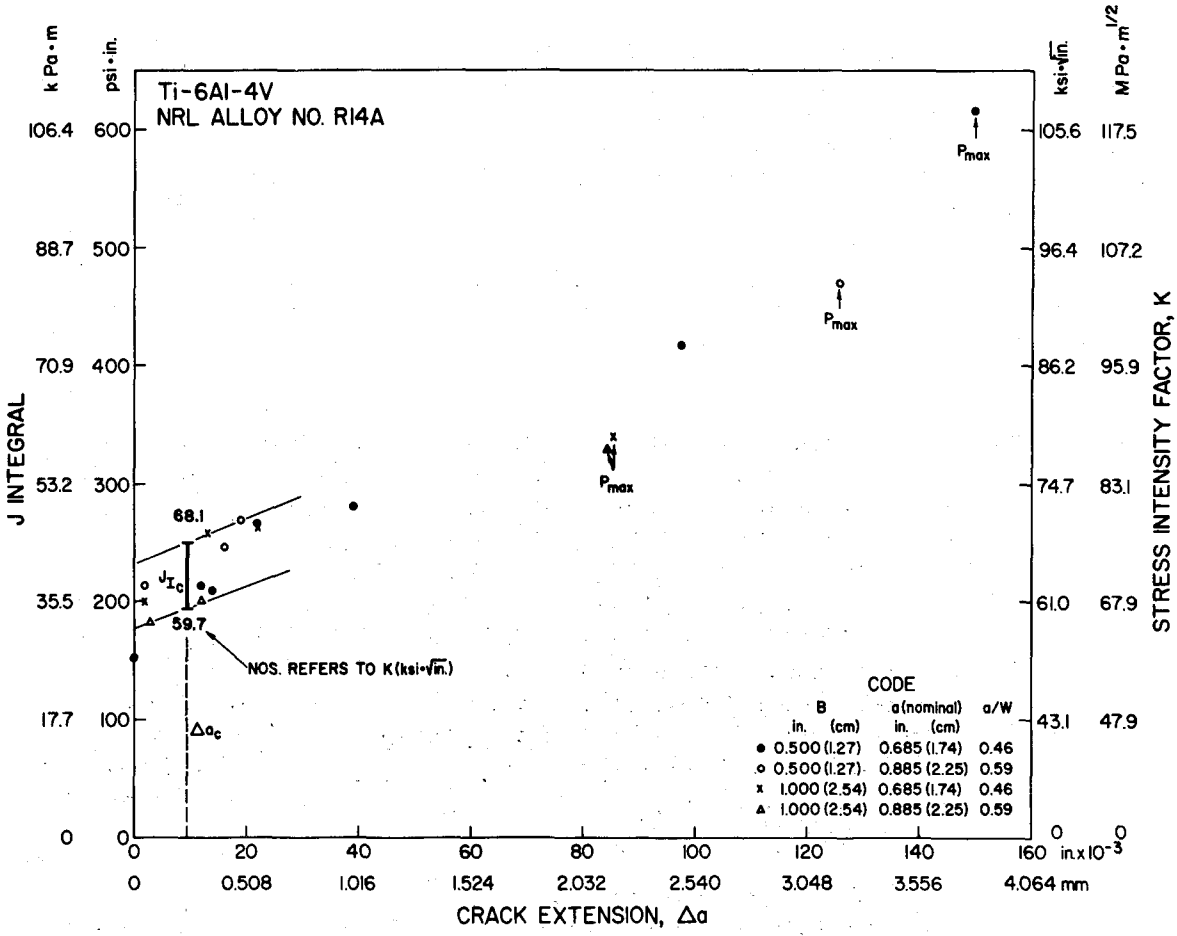

Fig. 11 — The J integral as a function of crack extension (Δa), showing its independence of thickness B and initial crack length a of elastic-plastic specimens. The critical value of J_{Ic} for initiation of crack extension is determined by Δa_c.

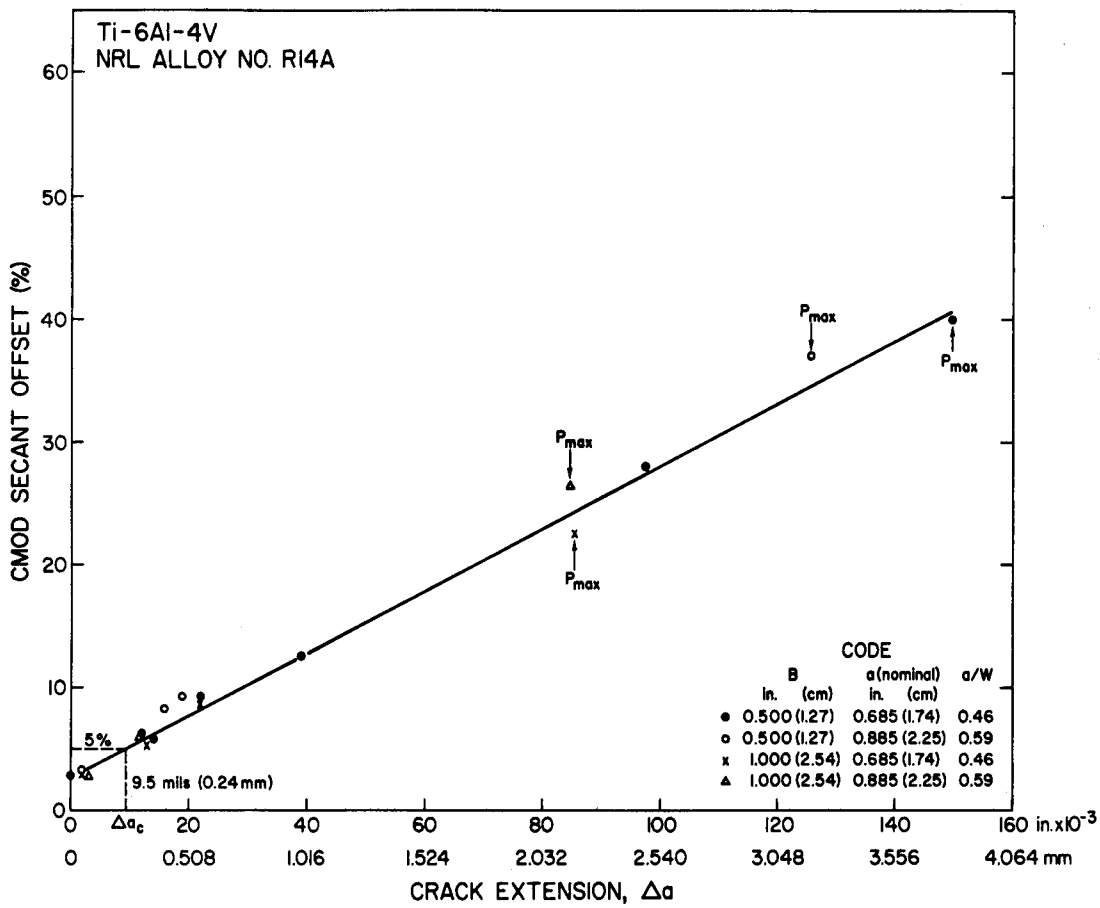

Fig. 12 — Percent secant offset in the crack mouth opening deflection (CMOD). This is directly proportional to crack extension Δa and appears independent of thickness B and crack length a. The 5% CMOD secant offset is used to define Δa_c, the amount of crack extension corresponding to initiation; Δa_c in turn is used to infer the critical value J_{Ic} in Fig. 11.

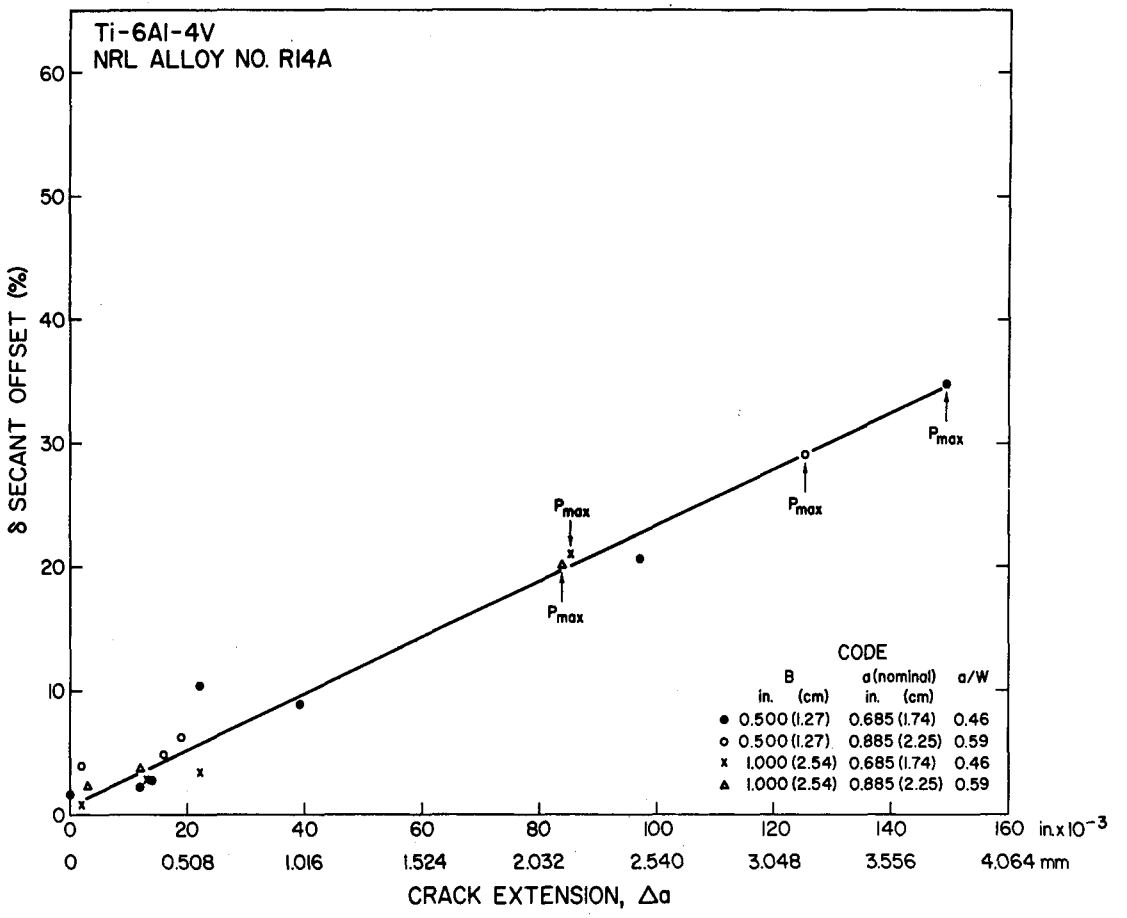

Fig. 13 — Percent secant offset in displacement δ, at the point of unloading, as a function of crack extension Δa

Percent Crack Extension as a Criterion for Initiation

The point of initiation of crack extension might well be defined in terms of some small increment of crack extension, say 1 or 2% of the initial crack length, or perhaps an extrapolation of the data to 0% extension. These criteria are examined in Fig. 14, where J integral values are plotted as a function of percent crack extension. Again, as in Fig. 11, J appears independent of thickness and initial crack length. For a 1%-extension criterion J_{Ic} would appear to lie between 190 and 252 psi · in. (33.7 and 44.7 kPa·m); for 2% extension J_{Ic} would appear to lie between 203 and 266 psi · in. (36.0 and 47.2 kPa·m); and, if the data are extrapolated to 0% extension, a value of J_{Ic} between 177 and 239 psi · in. (31.4 and 42.4 kPa·m) is inferred. Again it appears that J_{Ic} determined at initiation is only about 1/3 of the value implied had displacement at maximum load been used.

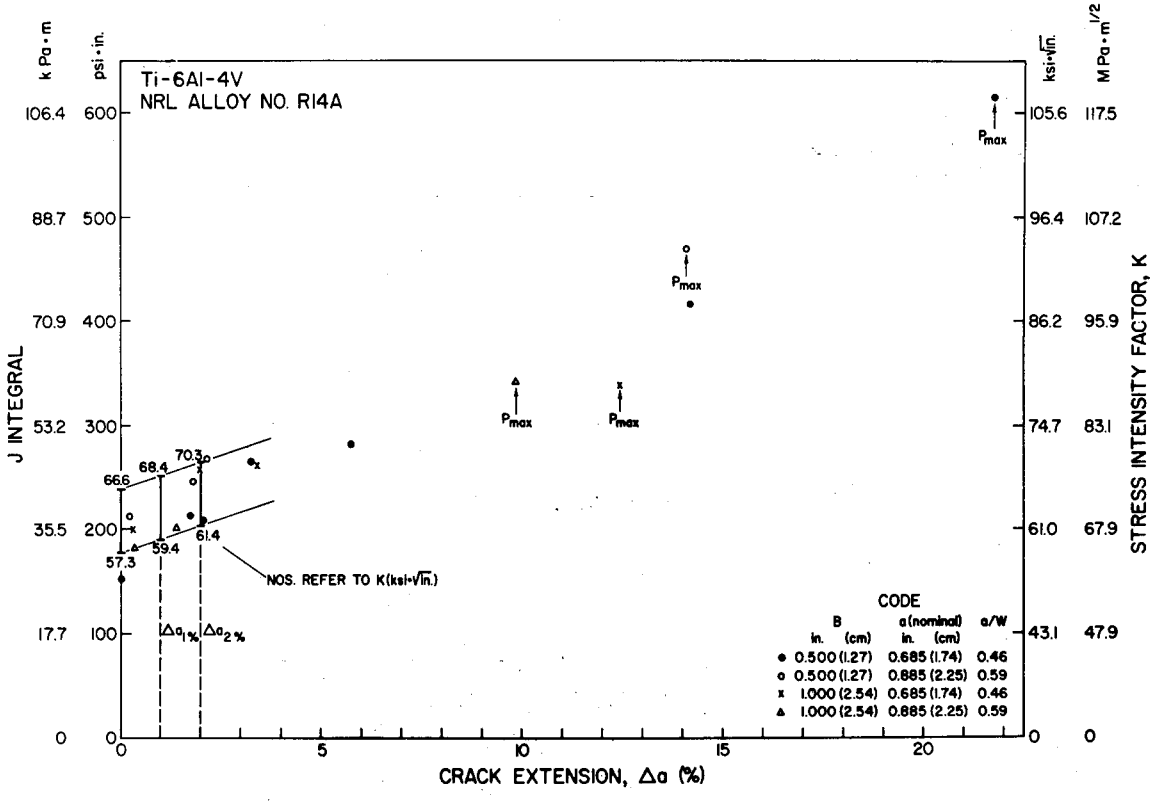

Fig. 14 — The J integral plotted as a function of *percent* crack extension. This appears to be independent of thickness and initial crack length of elastic-plastic specimens. J_{Ic} is indicated (in terms of the K translation values) for 0, 1 and 2% extension.

These data are summarized in Tables 3 and 4 together with data from the previous section and with the respective K_{Ic} translations (via $J_{Ic} = K_{Ic}^2/E$). It would appear that the choice of initiation criterion does not materially affect the value of J_{Ic}, and, to reiterate, it would appear that the uncertainty in J_{Ic} and K_{Ic} (Table 4), is of similar order as the toughness variation expected in the plate itself.

Table 3
Summary of J-Integral Data on Specimens of Ti-6Al-4V
(NRL Alloy R14A)

Specimen No.	Initial Crack Length, a (in.)				Crack Extension Δa (in.)				Crack Extension (%)	J(a) (psi-in.)	δ (10^{-3} in.)	δ Secant Offset (%)	CMOD (10^{-3} in.)	CMOD Secant Offset (%)	Comments	a + Δa (in.)	J(a + Δa) (psi-in.)
	1/4 B	1/2 B	3/4 B	Av.	1/4 B	1/2 B	3/4 B	Av.									
Thickness B = 0.5 in.; Nominal a = 0.685 in.																	
22	0.685	0.687	0.679	0.684	–	–	–	–	–	152	18.3	1.7	12.1	2.8		0.684	152
23	0.685	0.697	0.697	0.693	0.028	0.005	0.003	0.012	1.73	213	22.0	2.3	14.2	6.2		0.705	213
27	0.677	0.684	0.680	0.680	0.021	0.012	0.008	0.014	2.06	209	21.8	2.8	14.5	5.8		0.694	209
24	0.685	0.685	0.675	0.682	0.007	0.013	0.047	0.022	3.23	266	24.9	10.5	16.4	9.3		0.704	266
25	0.681	0.684	0.677	0.681	0.025	0.041	0.050	0.039	5.73	281	25.6	9.0	17.2	12.6		0.720	281
18	0.680	0.689	0.684	0.684	0.099	0.099	0.094	0.097	14.18	418	31.5	20.9	22.9	28.0		0.781	391
21	0.684	0.690	0.682	0.685	0.136	0.177	0.134	0.149	21.75	617	39.0	35.0	28.5	40.0	P_{max}	0.834	547
Thickness B = 0.5 in.; Nominal a = 0.885 in.																	
32	0.886	0.885	0.873	0.881	0.002	0.002	0.003	0.002	0.23	213	24.6	4.0	18.5	3.2		0.883	213
17	0.886	0.892	0.887	0.888	0.021	0.011	0.016	0.016	1.80	247	26.6	4.9	21.3	8.3		0.904	230
19	0.877	0.885	0.882	0.881	0.011	0.010	0.035	0.019	2.16	269	27.9	6.3	21.0	9.4		0.900	256
26	0.881	0.890	0.890	0.887	0.131	0.137	0.108	0.125	14.09	471	38.2	29.3	32.3	37.0	P_{max}	1.012	370
Thickness B = 1 in.; Nominal a = 0.685 in.																	
31	0.641	0.659	0.644	0.648	0.003	–	0.002	0.002	0.31	200	21.3	0.8	11.1	3.0		0.650	200
8A	0.644	0.671	0.663	0.659	0.033	0.002	0.004	0.013	1.97	258	24.5	2.8	13.8	6.3		0.672	258
34	0.648	0.656	0.633	0.646	0.010	0.005	0.050	0.022	3.41	263	24.7	3.4	12.8	8.7		0.668	263
15	0.681	0.695	0.676	0.684	0.120	0.034	0.101	0.085	12.43	340	28.3	21.2	18.8	22.5	P_{max}	0.769	324
Thickness B = 1 in.; Nominal a = 0.885 in.																	
9A	0.859	0.863	0.847	0.856	0.004	–	0.004	0.003	0.35	182	22.3	2.4	15.3	2.8		0.859	182
38	0.864	0.874	0.864	0.867	0.007	0.002	0.028	0.012	1.38	201	23.6	3.8	17.0	6.1		0.879	198
29	0.850	0.862	0.852	0.855	0.102	0.049	0.100	0.084	9.82	330	30.3	20.3	22.9	26.5	P_{max}	0.939	274

Metric Conversion: 1.00 in. = 2.54 cm; 1.00 psi-in. = 177.3 Pa·m.

Table 4
Comparison of J_{Ic} Values as a Function of Initiation Criterion

Criterion	J_{Ic} (psi · in.)		K_{Ic} (ksi · $\sqrt{in.}$)		$J_{Ic}(a + \Delta a)$ (psi · in.)		$K_{Ic}(a + \Delta a)$ (ksi · $\sqrt{in.}$)	
	Max	Min	Max	Min	Max	Min	Max	Min
1. 5% CMOD secant offset, Δa_c	250	192	68.1	59.7	–	–	–	–
2. Extrapolation of J vs. percent Δa to 0% Δa	239	177	66.6	57.3	239	178	66.6	57.5
3. Δa (1%)	252	190	68.4	59.4	248	188	67.9	59.1
4. Δa (2%)	266	203	70.3	61.4	258	198	69.2	60.6

NOTE (1): J_{Ic} = 192 psi-in. (K_{Ic} = 59.7 ksi · $\sqrt{in.}$), obtained from a valid K_{Ic} test.
NOTE (2): Translation J = G = K^2/E is assumed.
NOTE (3): Metric conversion: 1 ksi · $\sqrt{in.}$ = 1.112 MPa·$m^{1/2}$; 1 psi · in. = 177.3 Pa-m.

Evaluation of the J Integral Based on Crack Length at Unloading

Although J may not be a meaningful parameter after the initiation of crack extension, the behavior of J as a function of percent crack extension has been examined for the case where J is based on the crack length at the point of unloading instead of the length of the original fatigue percrack. Data treated in this fashion appear in Fig. 15 vs percent crack extension, as well as in Table 4; they are designated by $J_{Ic}(a + \Delta a)$ and $K_{Ic}(a + \Delta a)$. It is evident that the data near the point of initiation are not affected by this procedure; however data at P_{max} are lowered somewhat on the J scale, although to nowhere near the initiation level.

Comparison of $J_{Ic}(\Delta a)$ with $J_{Ic}(K_{Ic})$

Load-versus-CMOD records for the 1-in.-thick specimens (B = 1.000 in. = 2.54 cm) with $(a/W)_{nominal}$ = 0.46 have been examined to determine the stress-intensity factor K_Q. As shown in Table 5, two of three such records so analyzed yield ASTM-invalid K_Q numbers, as the criterion $P_{max}/P_Q \leqslant 1.10$ is violated. This suggests that the specimens with B ≐ 1.000 in. (2.54 cm) and a = 0.685 in. (1.74 cm) are elastic-plastic to only a marginal extent. On the other hand, specimens of only half this thickness, namely, B = 0.500 in. (1.27 cm), are much more elastic-plastic in behavior, as indicated by the ratio P_{max}/P_Q = 1.23 given in Table 5.

For the 1-in.-thick specimens (Table 5) the single K_Q number which is ASTM-valid (although only marginally so, since P_{max}/P_Q = 1.09), provides a value of K_{Ic} = 59.7 ksi·$\sqrt{in.}$ (66.4 MPa·$m^{1/2}$). If the conversion J = G = K^2/E is applied, this value of K_{Ic} translates to $J_{Ic}(K_{Ic})$ = 192 psi·in. (= 34.0 kPa·m), which is in good agreement with the values of J_{Ic} and K_{Ic} listed in Table 4.

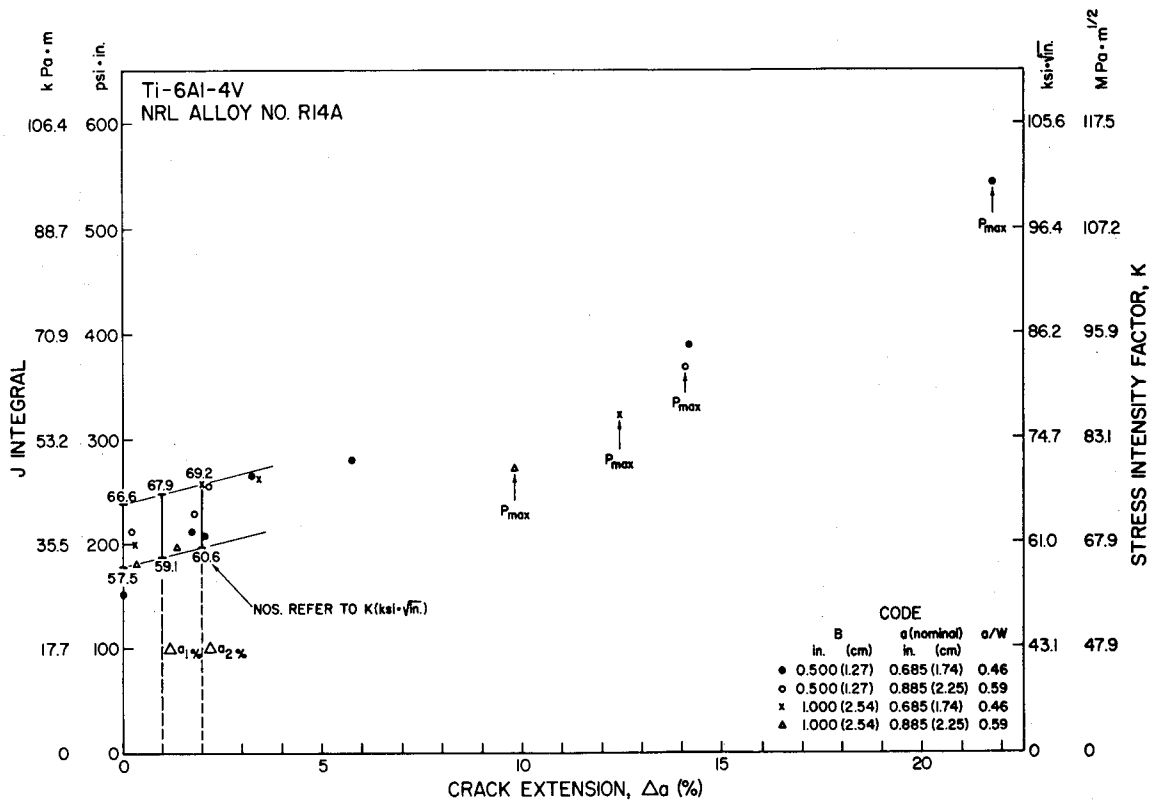

Fig. 15 — J integral, as a function of percent crack extension, for J referenced to the crack length a + Δa at unloading

Table 5
Stress Intensity Factor Data

Specimen No.	B (in.)	W (in.)	Initial Crack Length, a (in.) 1/4 B	1/2 B	3/4 B	Av.	a/W	P_{max} (lb)	P_Q (lb)	$\frac{P_{max}}{P_Q}$	K_Q (ksi · $\sqrt{in.}$)	2.5 $(K_Q/\sigma_{ys})^2 < B$, a, W − a	$K_Q = K_{Ic}$	J_{Ic} (K_{Ic}) psi · in.
Thickness B = 1 in.; Nominal a = 0.685 in.														
8	1.001	1.500	0.667	0.684	0.670	0.674	0.449	8660	7770	1.12	–	–	No	–
15	1.001	1.499	0.681	0.695	0.676	0.684	0.456	8600	7890	1.09	59.7	Yes	Yes	192
30	0.999	1.500	0.654	0.669	0.649	0.657	0.438	8760	7920	1.11	–	–	No	–
Thickness B = 0.5 in.; Nominal a = 0.685 in.														
21	0.501	1.501	0.684	0.690	0.682	0.685	0.456	4975	4030	1.23	–	–	No	–

Metric conversion: 1 in. = 2.54 cm; 1 lb (force) = 4.445 N; 1 ksi·$\sqrt{in.}$ = 1.112 MPa·$m^{1/2}$.
1 psi·in. = 177.3 Pa·m.

Initiation and the Loading Curve

Displacement δ and CMOD are plotted in Fig. 16 as a function of crack extension Δa. In general, it appears that these data separate on the basis of crack length a and specimen thickness B. If the value Δa_c = 9.5 mils (0.24 mm) is used to define initiation, (Figs. 11 and 12), then values of critical displacement δ_c for initiation can be inferred from Fig. 16 for the various sets of B and a. These values of δ_c (Δa_c) are indicated in the respective load-versus-displacement diagrams of Fig. 6. These points appear to fall reasonably near the points at which the calculated loading curves deviate from those of the precracked specimens.

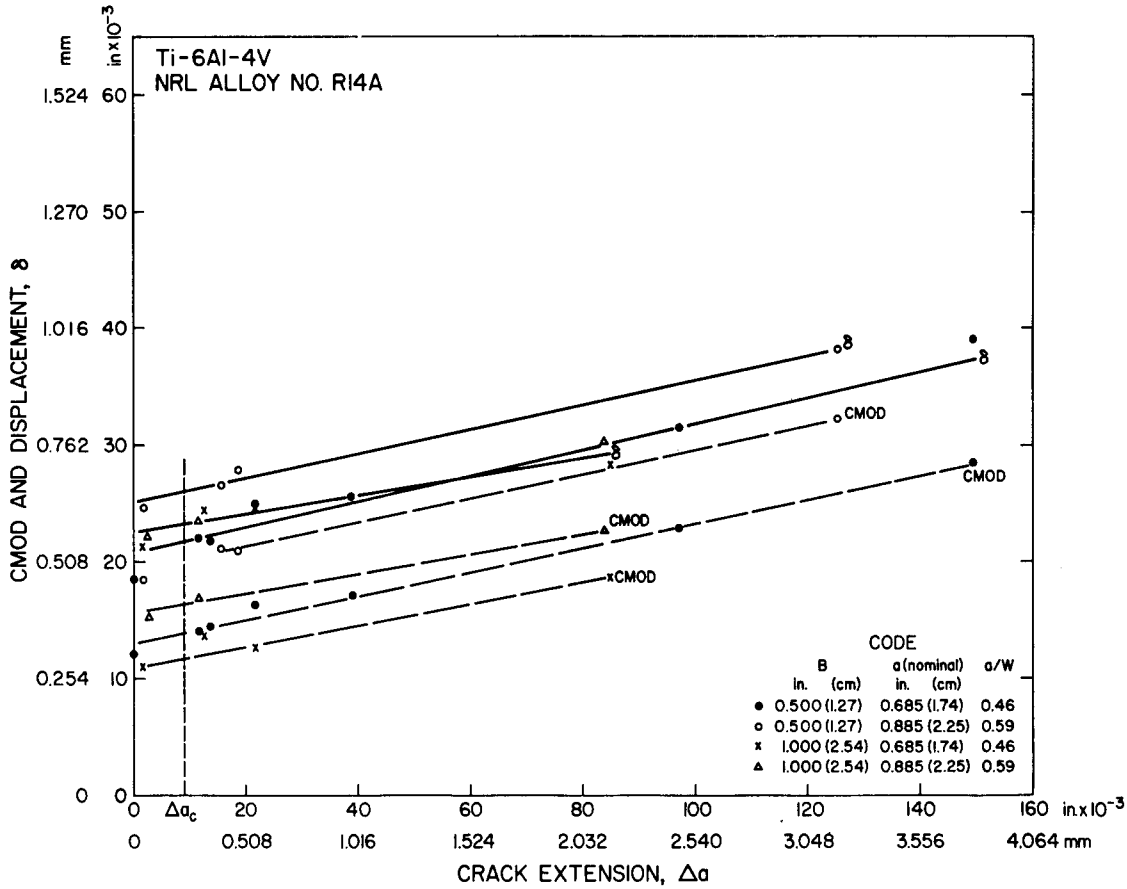

Fig. 16 — Displacement δ and crack mouth opening deflection CMOD as a function of crack extension Δa.

SUMMARY

The J integral has been examined as a criterion for the initiation of crack extension in specimens of an alloy for which crack extension occurs long before maximum load. The Ti-6Al-4V alloy selected is known to be susceptible to the sustained-load-cracking form of subcritical crack growth. Four types of three-point bend specimens were employed: of two different thicknesses (B = 0.5 and 1.0 in.) and two crack lengths (a = 0.685 and

0.885 in.). These fatigue-precracked specimens exhibited, to varying degrees, loading behavior characteristic of the lower end of the elastic-plastic regime. That is, all exhibited limit loads which were only a fraction of those expected for the fully plastic state; further, behavior of the specimen type with the most highly constrained crack appeared to be only marginally elastic-plastic, because only one specimen of three of this type (B = 1.0 in. and a = 0.685 in.) examined for K_Q provided an ASTM-valid K_{Ic} value.

For each specimen type, values of the J integral were obtained as a function of crack extension. Values of the J integral were determined on the basis of a compliance-type calibration which used the plane-stress solutions of Bucci et al. These solutions were found to simulate well the loading curves of the fatigue-precracked specimens. For each specimen type, crack extensions were defined by unloading duplicate specimens from various points on the load-displacement diagram and heat tinting.

Results from this study appear favorable to a J_{Ic} criterion for the initiation of crack extension. Specifically, the results from all four specimen types suggest that:

- The J-integral value associated with a given amount of crack extension is independent of specimen thickness and initial crack length.

- Crack extension, when taken as an average of values measured at the quarterpoints of specimen thickness, appears to be a useful parameter for defining initiation.

- For various criteria examined for the initiation of crack extension, the resultant J_{Ic} values are in good agreement with the K_{Ic} value noted above. These criteria include percent crack extension (0, 1 and 2%) as well as an absolute extension defined by the secant offset in the crack mouth opening deflection (CMOD).

- The percent CMOD secant offset is directly proportional to the amount of crack extension, independent of specimen thickness and crack length.

- The percent secant offset in the displacement δ does not appear to correlate well with crack extension.

- For determining J_{Ic} at initiation, it appears to make negligible difference whether J values are determined from the original or instantaneous crack length.

- The J_{Ic} value determined for initiation is only about 1/3 of that implied if maximum load were assumed blindly as the initiation criterion for this alloy.

ACKNOWLEDGMENTS

The authors gratefully acknowledge Mr. S. J. McKaye for very able technical assistance and the Office of Naval Research for financial support. Special thanks are extended to Drs. G. R. Irwin and F. J. Loss for stimulating discussions during the evolution of this work.

REFERENCES

1. J.R. Rice, "A Path Independent Integral and the Approximate Analysis of Strain Concentration by Notches and Cracks," Trans. ASME, Series E, J. Applied Mechanics 35 (1968) 379-386.
2. E399-72, "Standard Method of Test for Plane-Strain Fracture Toughness of Metallic Materials," *1972 Annual Book of ASTM Standards*, Part 31, Am. Soc. Testing Mat., Philadelphia, 1972, pp. 955-974.
3. G.R. Irwin, "Fracture Mechanics," in *Structural Mechanics*, Proc. of First Symposium on Naval Structural Mechanics, J.N. Goodier and N.J. Hoff, editors Pergamon Press, New York, 1960, pp. 557-594.
4. J.E. Srawley, "Evaluation of J for Threepoint Bend Tests," presented at joint meeting of the Task Group on Fracture Mechanics and Task Group E-24.01.09 on the J Integral, both of ASTM Committee E-24, Harvard University, Sept. 12, 1972.
5. A.S. Kobayashi, S.T. Chiu, and R. Beeuwkes, "A Numerical and Experimental Investigation on the Use of J-Integral," Engineering Fracture Mechanics 5 (1973) 293-305.
6. J.S. Ke and H.W. Liu, "The Measurement of Fracture Toughness of Ductile Materials," Engineering Fracture Mechanics 5 (1973) 187-202.
7. D.E. McCabe, Armco Steel Corporation, Research Center, Middletown, Ohio, personal communication, 1973.
8. J.A. Begley and J.D. Landes, "The J Integral as a Fracture Criterion," *Fracture Toughness*, Proc. 1971 Nat. Symp. on Frac. Mech., Part II, ASTM STP 514, Am. Soc. Testing Mat., Philadelphia, 1972, pp. 1-20.
9. J.D. Landes and J.A. Begley, "The Effect of Specimen Geometry on J_{Ic}," *Fracture Toughness*, Proc. 1971 Nat. Symp. on Frac. Mech., Part II, ASTM STP 514, Am. Soc. Testing Mat., Philadelphia, 1972, pp. 24-39.
10. G.R. Yoder, C.A. Griffis, and T.W. Crooker, "Sustained-Load Cracking of Titanium — A Survey of 6Al-4V Alloys," NRL Report 7596, Aug. 24, 1973.
11. J.R. Rice, "Mathematical Analysis in the Mechanics of Fracture," Chapter 3 in *Fracture*, H. Liebowitz, editor, Vol. II, Academic Press, New York, 1968, pp. 191-311.
12. G.R. Irwin, "Fracture Mechanics Characterizations and Fracture Toughness Measurements," paper presented at meeting of Am. Soc. Civil Eng., Cleveland, Apr. 1972, to be published in Trends in Engineering (Bombay, India).
13. J.L. Sanders, Jr., "On the Griffith-Irwin Fracture Theory," Trans. ASME, Series E, J. Applied Mechanics 27 (1960) 352-353.
14. G.R. Irwin, written discussion following Ref. 8, pp. 22-23.
15. G.R. Irwin and P.C. Paris, "Fundamental Aspects of Crack Growth and Fracture," Chapter 1 in *Fracture*, H. Liebowitz, editor, Vol. III, Academic Press, New York, 1971, pp. 1-46.
16. J.E. Srawley, "Plane Strain Fracture Toughness," Chapter 2 in *Fracture*, H. Liebowitz, editor, Vol. IV, Academic Press, New York, 1969, pp. 45-68.

17. R.J. Bucci, P.C. Paris, J.D. Landes, and J.R. Rice, "J Integral Estimation Procedures," *Fracture Toughness*, Proc. 1971 Nat. Symp. on Frac. Mech., Part II, ASTM STP 514, Am. Soc. Testing Mat., Philadelphia, 1972, pp. 40-69.

18. R.J. Goode, Naval Research Laboratory, personal communication, 1973.

NOMENCLATURE

a = crack length

B = thickness of specimen

CMOD = crack mouth opening deflection

E = Young's modulus

E_{tot} = total strain energy stored in a cracked bend bar at load P

G = crack extension force

G_{Ic} = critical value of G for initiation of crack extension

J = value of the J integral

J_{Ic} = critical value of the J integral for the initiation of crack extension

K = stress-intensity factor

K_{Ic} = critical value of stress-intensity factor for initiation of crack extension

K_Q = stress-intensity factor defined by ASTM-E399-72 5% secant offset method, determined from the load-vs-CMOD record

$\mathbf{n}$ = outward normal along Γ

P = applied load

P_{max} = maximum load

P_Q = load defined by ASTM-E399-72 5% secant offset method, determined from the load-vs-CMOD record

r_y = radius of plastic zone

S = span length

ds = increment of arc length along Γ

$\mathbf{T}$ = traction vector

U = potential energy per unit thickness

$\mathbf{u}$ = displacement vector

u,v = components of displacement $\mathbf{u}$ in x and y directions respectively

W = strain energy density; also depth of specimen

x,y = Cartesian coordinates emanating from the notch or crack tip

Γ = contour surrounding the notch or crack tip

δ = displacement

ϵ = strain

ν = Poisson's ratio

σ = stress

$\boldsymbol{\sigma}$ = stress tensor

σ_{ys} = yield stress

*U.S. GOVERNMENT PRINTING OFFICE:1974 542-171/Z-237 1-3